

Mosaic crystal algorithm for Monte Carlo

P. A. Seeger^{a,*}, L. L. Daemen^b

^a*239 Loma del Escolar, Los Alamos, NM 87544, USA*

^b*Manuel Lujan Jr. Neutron Scattering Center, Los Alamos National Laboratory, Los Alamos, NM 87545, USA*

Abstract

An algorithm is presented for calculating reflectivity, absorption, and scattering of mosaic crystals in Monte Carlo simulations of neutron instruments. The algorithm uses multistep transport through the crystal with an exact solution of the Darwin equations at each step. It relies on the kinematical model for Bragg reflection (with parameters adjusted to reproduce experimental data). For computation of thermal effects (the Debye-Waller factor and coherent inelastic scattering), an expansion of the Debye integral as a rapidly converging series of exponential terms is also presented. Any crystal geometry and plane orientation may be treated. The algorithm has been incorporated in the Neutron Instrument Simulation Package (NISP).

1. Introduction

We describe here a recent addition to the Neutron Instrument Simulation Package (NISP), namely a new algorithm for neutron transport in a mosaic crystal. Single crystals are commonly used by neutron scatterers to select particular neutron energies or to focus neutron beams. Therefore a good crystal model is an essential part of a Monte Carlo library for simulating neutron scattering instruments. Although the algorithm is presented in terms of an element in NISP, the source code is provided (as with all NISP modules) so that it may be adapted to other libraries and Monte Carlo programs.

Our purpose in developing NISP [1-4] is to provide the community of neutron scatterers with a general, versatile tool similar to what is available for optical design in other regimes. A graphical interface allows the user to produce a 3D model of the instrument by selecting optical elements from a list and defining their characteristics, location, and orientation in space. The code has a large collection of source terms, samples, and detectors. Magnetic induction regions may be defined and precession is computed. Users can add their own subroutines to model optical elements that are not in the library, either by modifying existing algorithms or adding their own to the library. The package is freely available on the web at <http://strider.lansce.lanl.gov/NISP/Welcome.html>. We welcome comments and requests for additions or changes, and we offer technical support to the extent that we have the time to do so.

*Corresponding author.

E-mail address: PASeeger@aol.com

2. Multiple-step neutron transport

Our algorithm transports neutrons stepwise through a crystal. We assume a fixed step length t , and treat that same t as a mosaic block size such that the mosaic deviations of the plane orientation from one step to the next are not correlated. Thus there is no explicit primary extinction in the algorithm; such an effect can only be approximated by modification of the parameters. All geometric effects, including mosaic spread, are treated externally as part of the neutron transport. There are several advantages to taking small steps instead of using an analytical solution for the total crystal thickness:

- The depth of the interaction(s) within the crystal is estimated
- “Walking” along the crystal due to multiple reflections is included
- Secondary extinction is included naturally
- The shape of the crystal is not limited to plane parallel surfaces.

The solution of the Darwin equations for reflection and transmission of neutrons in a crystal can be expressed analytically [5] in terms of three dimensionless parameters:

$$\begin{aligned}
 a &= \mu t \\
 b &= \sigma t \\
 \zeta &= \sin \phi / \sin \phi'
 \end{aligned}
 \tag{1}$$

where t is the path length through the crystal (or in our case through one mosaic block), μ is the macroscopic cross section (or cross section per unit volume, with dimensions of length) for all processes *except* Bragg scattering, σ is the macroscopic cross section for Bragg scattering, and the angles ϕ and ϕ' are measured from the crystal face respectively to the incident and reflected neutron beams. We treat every block as having the scattering planes either parallel (Bragg case) or perpendicular to (Laue case) the surface. In either case, $\zeta \equiv 1$.

Having selected t , the solution for absorbtivity A , reflectivity R , and transmissivity T in the thin-crystal limit is

$$\begin{aligned}
 A &= a = \mu t \\
 R &= b = \sigma t \\
 T &= 1 - R - A .
 \end{aligned}
 \tag{2}$$

There is no first-order contribution from the geometric parameter ζ , and the same result is obtained for either Bragg (reflection) or Laue (transmission) geometry.

Using this limit would lead to many steps in the crystal, with the advantage that every neutron samples many mosaic blocks and the motion within the crystal is more precise, but with the disadvantage of long execution times in a Monte Carlo simulation. Even when the step is small, however, it will happen that T becomes too small to use the thin-crystal limit. We then use the full analytic solution from [5] with $\zeta = 1$. For Bragg (reflection) geometry,

$$\begin{aligned}
 p &= a + b, \quad r = (a^2 + 2 a b)^{1/2} \\
 R &= b \sinh r / (r \cosh r + p \sinh r) \\
 T &= r / (r \cosh r + p \sinh r) \\
 A &= 1 - R - T .
 \end{aligned}
 \tag{3}$$

Or, for Laue (transmission) geometry,

$$\begin{aligned}
 R &= e^{-p} \sinh b \\
 T &= e^{-p} \cosh b \\
 A &= 1 - R - T.
 \end{aligned}
 \tag{4}$$

The code chooses which geometry to use based on the inclination of the crystal planes with respect to the entrance surface. If the inclination is neither 0 nor 90°, the mosaic blocks on the entrance and exit surfaces will not be accurate. In that case, or if the exit surface is not parallel to the entrance, a smaller value of t is recommended to minimize the error. There is no upper limit on t , since the solutions are exact. Note that if t is large enough to span the crystal, the point of interaction will be assumed to be halfway through and no secondary extinction will occur.

3. Bragg scattering cross section

The kinematical model is used to compute the Bragg scattering cross section [6]. The function $\sigma(\lambda, \theta)$ is expressed as a product of two terms:

$$\sigma(\lambda, \theta) = Q(\lambda) W(\theta - \theta_B), \theta
 \tag{5}$$

where $Q(\lambda)$ is determined by crystal structure and the mosaic function $W(\theta - \theta_B)$ (often called the “normalized rocking curve,” though as seen in Figure 1 it bears little resemblance to an actual rocking curve). In the kinematical model,

$$Q(\lambda) = \lambda^3 |F_{\text{hkl}}|^2 / V_0^2 \sin 2\theta_B,
 \tag{6}$$

where θ_B is the nominal Bragg angle (a function of λ), V_0 is the volume of the unit cell, d_{hkl} is the plane spacing, and F_{hkl} is the unit-cell structure factor including the Debye-Waller factor. Using the Bragg condition, $n \lambda = 2 d \sin \theta_B$, to replace one power of λ ,

$$Q(\lambda) = \lambda^2 d_{\text{hkl}} |F_{\text{hkl}}|^2 / (n V_0^2 \cos \theta_B),
 \tag{7}$$

where n is the order number. For any particular crystal planes, such as Si(111), we choose a value of step size t and tabulate a value S (\AA^{-2}) representing

$$S = t d_{\text{hkl}} (|F_{\text{hkl}}| \exp(W_{\text{hkl}}) / V_0)^2.
 \tag{8}$$

Note that the Debye-Waller factor $\exp(-W_{\text{hkl}})$ has been removed from the structure factor, and the temperature of the crystal may be varied by recomputing W_{hkl} as described in the following section. If experimental data are available, we may choose the value of S to fit the reflectivity data rather than the crystallographic parameters. The dimensionless reflectivity per step (averaged over the mosaic distribution) is then

$$b = \sigma t = \lambda^2 S \exp(-2 W_{\text{hkl}}) / (n \cos \theta_B).
 \tag{9}$$

In this equation we choose n as a function of θ , the actual angle of incidence of the neutron, to minimize $|\theta - \theta_B|$. The (Gaussian) mosaic distribution $W(\theta - \theta_B)$ is treated by Monte Carlo integration.

It must be noted that the expressions for $Q(\lambda)$ have a singularity at $\lambda = 2 d_{\text{hkl}}$, for which $\theta_B = 90^\circ$. Thus the condition $R \ll 1$ can not be met, and thus *the kinematical model is not*

valid for backscattering. Although the singularity is very narrow, in a simulation of a backscattering analyzer neutrons will occasionally fall into it. We have taken the expedient of placing an arbitrary lower limit on $\cos\theta_B$ when used in the denominator, corresponding to an angle 1° off normal. Also note that the kinematical model does not include primary extinction.

4. Debye-Waller factor

In order to calculate the Debye-Waller factor as a function of temperature we must know the mean quadratic displacement of all atoms in the material. This problem is difficult to solve in its complete generality and several drastic approximations are usually made. As described by Guinier [7], the motion of atoms in a simple crystal lattice containing N atoms is considered the superposition of $3N$ harmonic waves propagating in the material. In the approximation of Debye, the $3N$ waves have a frequency distributed quadratically between zero and a maximum frequency, ν_m , such that $h \nu_m = k \Theta_D$, where Θ_D is a material-dependent parameter known as the Debye temperature, h is Planck's constant, and k is Boltzmann's constant. One can then show [7] that the mean quadratic displacement of atoms in the crystal is given by:

$$u_0^2 = \frac{3h^2}{4\pi^2 M k \Theta_D} \left[\frac{1}{4} + \frac{T}{\Theta_D} \varphi\left(\frac{\Theta_D}{T}\right) \right], \quad (10)$$

where

$$\varphi(x) = \frac{1}{x} \int_0^x \frac{t}{\exp t - 1} dt \quad (11)$$

is the Debye integral, T is the crystal temperature, and M is the mass of the vibrating atom. Note that for non-cubic crystals the relevant component of u_0 is perpendicular to the reflecting planes. Once u_0 is known, the Debye-Waller exponent is easily calculated [8]:

$$2 W_{\text{hkl}} = (4 \pi u_0 \sin \theta_B / \lambda)^2 = (2 \pi u_0 / d_{\text{hkl}})^2. \quad (12)$$

Tables exist for the Debye integral, but a closed analytic form is preferred. A number of power series expansions have been proposed [7], but they converge rather slowly. Here we propose a new expansion of eq. (11) in a rapidly converging series of exponential functions. Since Θ_D/T is a positive quantity, the integration variable t is always positive, and $\exp(-t)$ is always smaller than unity. It follows that

$$\frac{1}{\exp t - 1} = \frac{\exp(-t)}{1 - \exp(-t)} = \sum_{j=0}^{\infty} [\exp(-t)]^{(j+1)} = \sum_{j=1}^{\infty} \exp(-jt). \quad (13)$$

The integral is now a sum of terms of the form $t \exp(-jt)$, which can be integrated by parts. The final result is

$$\varphi(x) = \frac{1}{x} \left[\frac{\pi^2}{6} - \sum_{j=1}^{\infty} \left(\frac{x}{j} + \frac{1}{j^2} \right) \cdot \exp(-jx) \right], \quad (14)$$

where the summation for the lower limit has been evaluated using [9]

$$\sum_{j=1}^{\infty} \frac{1}{j^2} = \zeta(2) = \frac{\pi^2}{6}. \quad (15)$$

In this relation, ζ is the Riemann zeta function. Then

$$W_{hkl} = \frac{2873 \text{ \AA}^2 \text{ amu K}}{d_{hkl}^2 M \Theta_D} \left\{ \frac{1}{4} + \left(\frac{1}{\xi^2} \right) \left(\frac{\pi^2}{6} - \exp(-\xi) \left[\xi + 1 + \exp(-\xi) \left(\frac{\xi}{2} + \frac{1}{4} + \dots \right) \right] \right) \right\}, \quad (16)$$

where $\xi = \Theta_D/T$. The series converges rapidly for $T < \Theta_D$, requiring only two terms to get error $< 0.2\%$ for any $\xi > 2$. For higher precision at higher T , we truncate the sum when a term is less than 0.01, and treat the residual terms as the sum of a geometric series with the ratio equal to the ratio of the last 2 computed terms. Then as a worst case, Pb at room temperature with $\xi = 0.36$, seven terms are included and the error is 0.4%.

5. Absorption cross sections

The absorption coefficient μ includes three effects: incoherent scattering, nuclear absorption, and coherent inelastic scattering. These are taken directly from Appendix A3 of [5]. The absorbtivity coefficient is

$$a = \mu t = t [\mu_i + \mu_{a0} \lambda + \mu_c f(x)] \quad (17)$$

The incoherent scattering absorption, μ_i , is taken to be independent of λ , and the nuclear absorption is assumed proportional to λ with value μ_{a0} at $\lambda = 1 \text{ \AA}$. Because of the λ -dependence, the nuclear absorption becomes important at long wavelengths. The dominant absorption at short wavelengths is the coherent inelastic (phonon) term, represented by the coherent scattering macroscopic cross section μ_c and an ‘‘Einstein-like’’ model for the lattice vibrations:

$$f(x) = 1 - \{ [1 - \exp(-x)] / x \}, \quad (18)$$

in which

$$x = (4 \pi u_0 / \lambda)^2, \quad (19)$$

and u_0 (\AA) is the root-mean-square displacement of the atoms as computed above. For most crystals used as monochromators or analyzers (the exception being Pb), the temperature dependence of the scattering is much more significant than the DebyeWaller factor. Thus we may need to choose an effective value of Θ_D to give the correct u_0 .

6. Evaluating coefficients

Values of t and S for a number of common monochromator crystals are shown in Table 1. (When non-symmetrical crystals are included in a problem, the values of t and S must be made smaller.) For the example of Si(111), we chose $t = 0.2 \text{ cm}$. Taking the lattice constant to be 5.4309 \AA and the bound coherent scattering length to be 1.1491 fm , then $d_{111} = 3.1355 \text{ \AA}$, $F_{111} = 2.3476 \times 10^{-12} \text{ cm}$ (excluding the DebyeWaller factor), and $V_0 = 160.16 \text{ \AA}^3$ (with 8 atoms per unit cell). From eq. (8) we find $S = 1.3473 \times 10^{-4} \text{ \AA}^{-2}$. For computation of the

Table 1. Crystal Parameters

ID	d (Å)	t (mm)	S (/Å ²)	Θ_D (K)	M (amu)	μ_c (/cm)	μ_i (/cm)	μ_a (th) (/cm)
'Al (111) '	2.33798	2.00	2.01939e-4	405	26.98	0.0901	0.0005	0.0139
'Al (200) '	2.02475	2.00	1.74884e-4	405	26.98	0.0901	0.0005	0.0139
'Al (220) '	1.43172	2.00	1.23662e-4	405	26.98	0.0901	0.0005	0.0139
'Al (311) '	1.22097	2.00	1.05459e-4	405	26.98	0.0901	0.0005	0.0139
'Be (100) '	1.97956	0.10	1.83157e-4	955	9.01	0.9409	0.0002	0.0009
'Be (002) '	1.79215	0.10	3.31634e-4	955	9.01	0.9409	0.0002	0.0009
'Be (101) '	1.73285	0.10	2.77700e-4	955	9.01	0.9409	0.0002	0.0009
'Be (110) '	1.14290	0.10	1.22925e-4	955	9.01	0.9409	0.0002	0.0009
'Cu (111) '	2.08706	0.20	1.76995e-4	315	63.55	0.6338	0.0466	0.3201
'Cu (200) '	1.87045	0.20	1.53282e-4	315	63.55	0.6338	0.0466	0.3201
'Cu (220) '	1.27806	0.20	1.08387e-4	315	63.55	0.6338	0.0466	0.3201
'Cu (311) '	1.08993	0.20	0.92433e-4	315	63.55	0.6338	0.0466	0.3201
'Ge (111) '	3.26636	0.50	1.31150e-4	280	72.61	0.3719	0.0080	0.0972
'Ge (220) '	2.00023	0.50	1.13579e-4	280	72.61	0.3719	0.0080	0.0972
'Ge (311) '	1.70580	0.50	0.68491e-4	280	72.61	0.3719	0.0080	0.0972
'Ge (400) '	1.41438	0.50	0.80313e-4	280	72.61	0.3719	0.0080	0.0972
'PG (002) '	3.3539	0.20	1.805 e-4	420	12.01	0.6264	0.0001	0.0004
'Si (111) '	3.13553	2.00	1.34735e-4	500	28.09	0.1081	0.0002	0.0085
'Si (220) '	1.92011	2.00	1.16684e-4	500	28.09	0.1081	0.0002	0.0085
'Si (311) '	1.63748	2.00	0.70363e-4	500	28.09	0.1081	0.0002	0.0085
'Si (400) '	1.35772	2.00	0.82508e-4	500	28.09	0.1081	0.0002	0.0085

Debye-Waller factor and the lattice vibration term, values of the Debye temperature Θ_D and the atomic mass M are also given in the Table. All values of Θ_D (except for PG) have been reduced significantly from thermodynamic values in order to give the reported values of u_0 at $T = 295$ K. For instance, using $\Theta_D = 640$ K for Si would give $u_0 = 0.0648$ Å instead of the desired value of 0.081 Å. The exception, pyrolytic graphite (PG), has conflicting values in the literature, so Θ_D was left alone. The value of S for the PG(002) reflection was adjusted to reproduce a rocking curve reported by Shapiro [10]. The remaining columns in the table give the macroscopic absorption cross sections [8,11]. Note that μ_a (th) represents the absorption for thermal neutrons, $\lambda = 1.798$ Å.

When a user creates an instance of a “Mosaic Crystal” in the NISP web application, MC_Web, the location, orientation, geometric shape, asymmetry, mosaic spreads, and temperature of the crystal are entered in the first screen. The user also chooses one of the parameter sets (by identifier) from Table 1. Any of the parameters may be modified on a second screen; for instance, t and S may be changed for a different step size, or a completely different crystal may be defined. The MC_Web code computes the Debye-Waller factor and adjusts the attenuation factors for the step size, and generates a file of the parameters in the

form used in the NISP Monte Carlo program, MC_Run. Those parameters are $2d$ (Å), t (m), $S \exp(-2W)$ (Å⁻²), $4\pi u_0$ (Å), $t\mu_c$, $t\mu_i$, and $t\mu_a/1.798$ (Å⁻¹). For more information on using the program, visit the site at <http://strider.lansce.lanl.gov/NISP/Welcome.html>.

7. Examples

Figure 2 shows a comparison of the multiple-step Monte Carlo calculation (shown as points) to the analytical form (lines). The example is from Sears [8], and is a Si(111) crystal 1.0 cm thick. The orientation is varied to select specific wavelengths in both Bragg and Laue geometries, and the reflectivity is shown at the center of the rocking curve. The NISP code uses a Gaussian shape for the mosaic function $W(\theta - \theta_B)$. In order to match precisely the peak value used by Sears, $W(0) = 191.0$ per radian, the rms of the Gaussian was set to 2.09×10^{-3} radians (corresponding to a fwhm of 0.282°). Only one point, Bragg at 0.5 Å, is further from the line than its error bar. This example shows that the Monte Carlo integration faithfully reproduces the analytic solution.

Since PG is of primary importance in current simulations, rockingcurve peak and width estimates are shown in Fig. 3 as a function of neutron energy. The points on the figure are experimental data, read from Fig. 1 of [10]. The crystal parameters were adjusted to fit the data at 14 meV. Using the same parameters, we have computed the Bragg and non-Bragg attenuation as a function of incident angle at a neutron wavelength of 1.116 Å, for comparison to data of Fig. 6 of Grabcev [12], shown in Fig. 4. Details of the experiment were not reported, and we have estimated from the plot a triangular resolution function with a fwhm of 1° below and 1.5° above $\theta = 45^\circ$. The non-Bragg contribution and the intensities of the various orders of Bragg attenuation are in good agreement with the measurement. These comparisons show that the model behaves properly with respect to variations in wavelength and angle.

Acknowledgements

This work has been supported in part by the Manuel Lujan Jr. Neutron Scattering Center, a national user facility funded by the United States Department of Energy, Office of Basic Energy Sciences—Materials Science, under contract number W-7405-ENG-36 with the University of California.

References

- [1] P.A. Seeger, L.L. Daemen, R.P. Hjelm, and T.G. Thelliez, Proceedings of ICANSXIV, report ANL-98/33, 202 (1998).
- [2] L.L. Daemen, P.A. Seeger, T.G. Thelliez, and R.P. Hjelm, in “Neutrons and Numerical Methods-N2M” M.R.Johnson *et al.*, Eds., AIP Conference Proceedings 47 (1999) 41.
- [3] L.L. Daemen, P.A. Seeger, T.G. Thelliez, and R.P. Hjelm, SPIE Conference on “Radiation Sources and Radiation Interactions”, E.J.Morton, Ed., Proceedings of SPIE, Vol.3771 (1999) 80.

- [4] P. A. Seeger, T. G. Thelliez, and L. L. Daemen, "Neutron Instrument Simulation Package Users' Manual," <ftp://strider.lansce.lanl.gov/pub/NISP/document/Manual.pdf>.
- [5] V. F. Sears, *Acta Cryst.* **A53** (1997) 33.
- [6] V. F. Sears, "Neutron Optics," (Oxford University Press, New York, 1989) Ch. 5.
- [7] A. Guinier, "X-ray diffraction in crystals, imperfect crystals, and amorphous bodies," (Dover Publications Inc., New York, 1994), p.189.
- [8] V. F. Sears, *Acta Cryst.* **A53** (1999) 46.
- [9] I. S. Gradshteyn and I. M. Ryzhik, "Tables of integrals, series, and products," (Academic Press, Orlando, 1980) Eq.0.233.1.
- [10] S. M. Shapiro and N. J. Chesser, *Nucl. Inst. Methods* **101** (1972) 183.
- [11] V. F. Sears, *Neutron News* **3**(3) (1992) 26.
- [12] B. Grabcev, S. Todoreanu, and V. Cioca, *Nucl. Inst. Methods* **228** (1985) 465.

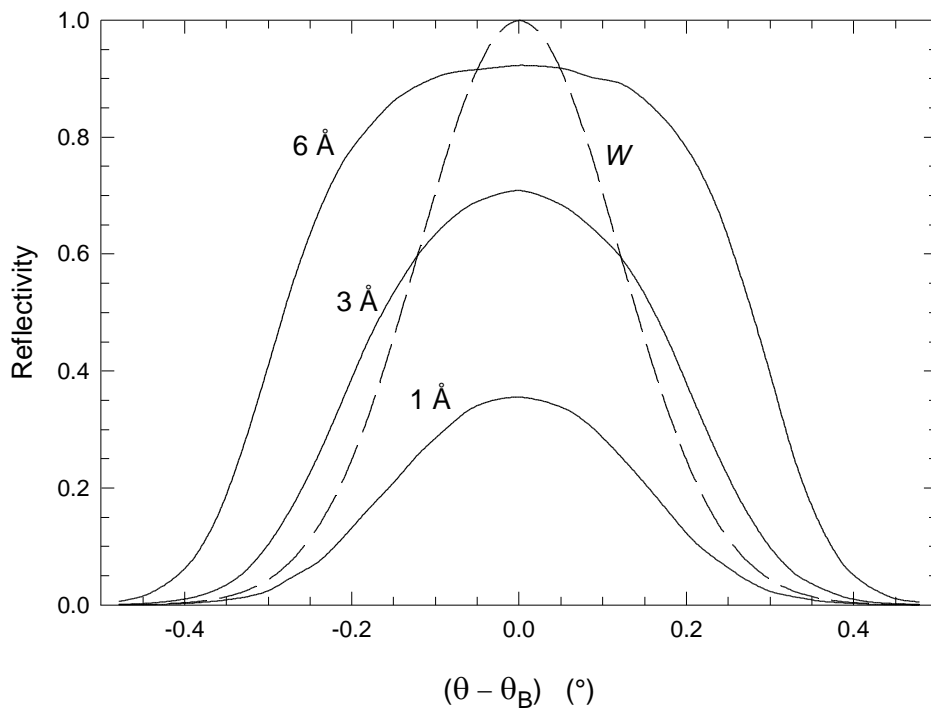


Fig. 1. Rocking curves computed for a Si (111) crystal, 1 cm thick, in reflection geometry. The "mosaic function" $W(\theta - \theta_B)$ is Gaussian, but the rocking curves are much flattened. The peaks of these curves are plotted in Fig. 2.

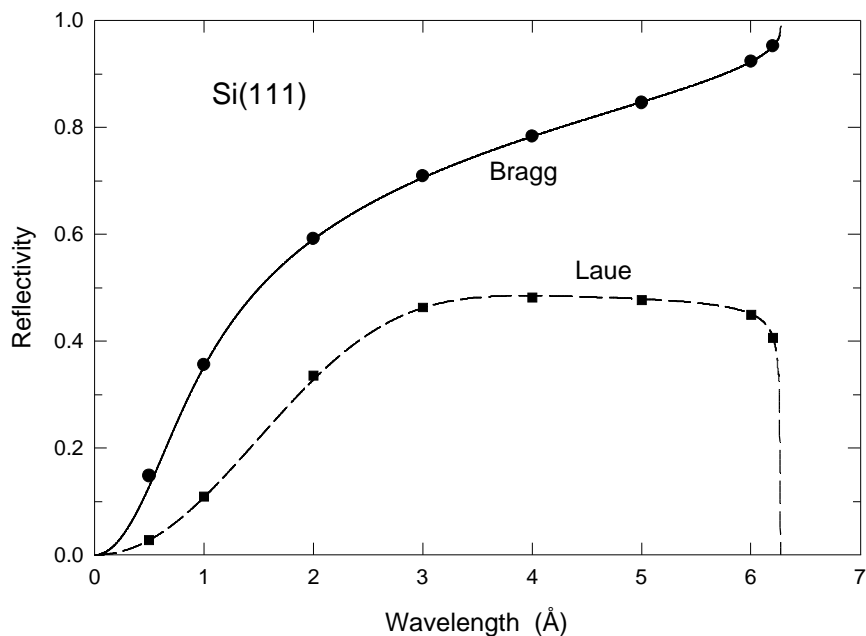


Fig. 2. Peak reflectivity as a function of wavelength for a 1.0-cm thick Si(111) crystal, in reflection (Bragg) and transmission (Laue) geometries. Lines are from the analytic expressions (3) and (4) for the full thickness of the crystal, and points are Monte Carlo simulations with step length 2.0 mm. Standard deviations of the points are comparable to the size of the symbols.

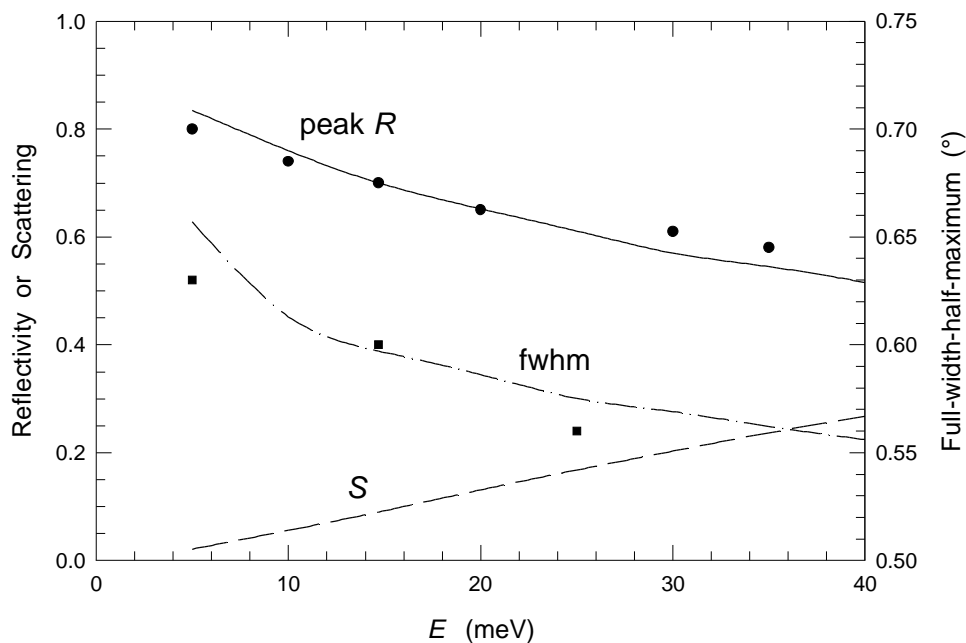


Fig. 3. Simulated peak reflectivity and width of rocking curves for a 0.22-cm thick PG(002) crystal in Bragg geometry, compared to experimental data from Shapiro [10]. The calculated energy-dependent inelastic scattering S is also plotted.

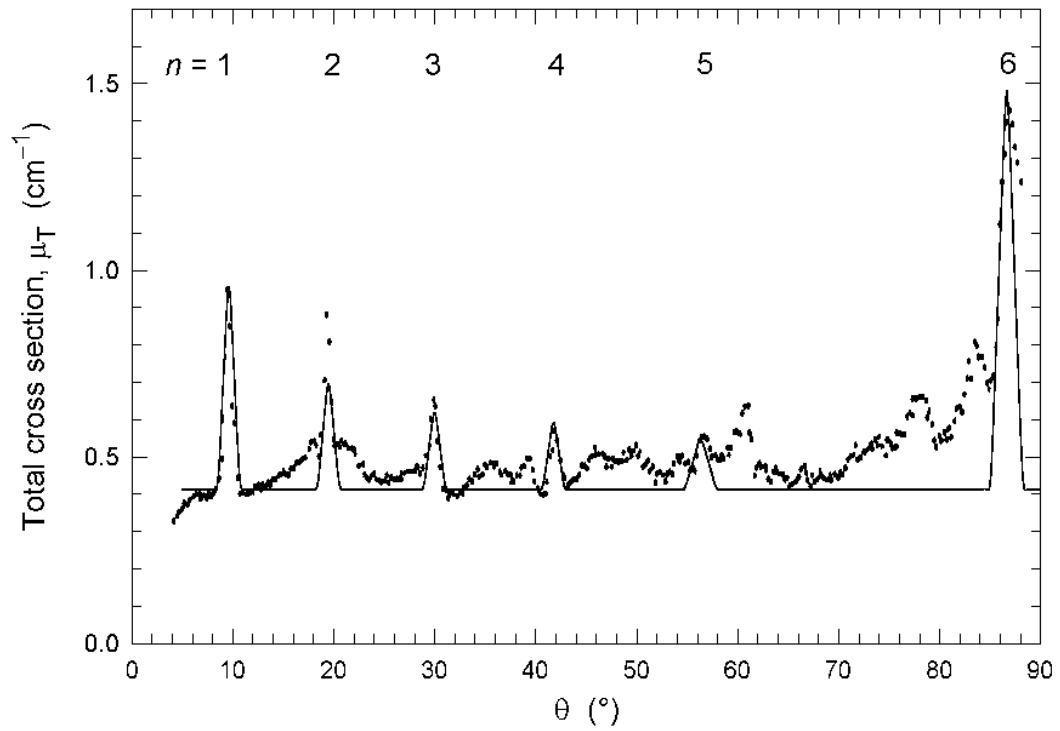


Fig. 4. Computed macroscopic total cross section for PG as a function of Bragg angle, for a neutron wavelength of 1.116 \AA . The data points are scanned from Fig. 6 of Grabcev [12].